Error localization and updating of junction properties for an engine cradle model

G. Vermot des Roches [1,2], **E. Balmes** [2,1], **S. Nacivet**[3]
[1]SDTools
44 rue Vergniaud, 75013, Paris, France
e-mail: **balmes@sdtools.com**

[2]Arts et Metiers ParisTech, PIMM
151 Boulevard de l'Hôpital, 75013, Paris, France

[3]PSA Groupe
92256 La Garenne Colombes Cedex, Paris, France

Abstract
Extending the bandwidth of validity of FEM models used in vibroacoustic design is a generic objective of model generation processes. Achieving this objective requires a critical review of both testing and modeling processes. Using the case study of an engine cradle, tools used to detect modal test inconsistencies are first illustrated. On the modeling side, weld spots and lines and variations of thickness due to press forming are shown to have relatively minor impact when compared to the contact surfaces. Usual junction simplifications are also shown to play a major role particularly at higher frequencies where more localized modeshapes occur.

1 Introduction

Extending the bandwidth of validity of FEM models used in vibroacoustic design is a generic objective of model generation processes at PSA Peugeot Citroën. Increasing this bandwidth implies a critical review of test/analysis correlation, focusing on both experimental errors and parameters having a visible influence on the vibration characteristics. Important aspects of such procedures will be illustrated on the sample case of an engine cradle shown in figure 1 using procedures implemented in the structural dynamics toolbox (SDT) [1] for MATLAB.

Figure 1: Engine cradle used as test case.

Test related errors are generally ignored in FEM updating procedures since their characterization is diffi-

cult. Classification strategies seeking to establish the reliability of experimental modeshapes and the localization of potential errors are addressed in section 2. The associated criteria are identification errors per mode/transfer, MIMO consistency and sorting of poorly correlated sensors with the MACCo. Once test results properly validated, modeshape expansion is shown to allow clearer identification of model parts where correlation needs improvement.

On the model side addressed in section 3, potential errors are found in the modeling of junctions, weld spots and lines as well as variations of geometry and thickness of press-formed parts. The first step of updating is a sensitivity study to the potential parameters and the study demonstrates that, at higher frequencies, usual simplifications of junctions may no longer be sufficient. Strategies to evaluate the impact of contact surfaces will be illustrated. Final updating results will be shown to lead to a classification of influent parameters that was not the initial expectation.

2 Classification of experimental errors

Test related errors are generally ignored in FEM updating procedures since their characterization is difficult. Classification strategies seeking to establish the reliability of experimental modeshapes and the localization of potential errors will first be addressed. The associated criteria are identification errors per mode/transfer, MIMO consistency and sorting of poorly correlated sensors with the MACCo. Once test results properly validated, modeshape expansion is shown to allow clearly identification of model parts where correlation needs improvement.

2.1 Localization of poor identification

It is well known that a difficulty in the use of stabilization diagrams is the good choice of modes within the result (since estimated modeshapes vary from order to order). In reality, the proper procedure is to use the stabilization result as a series of pole candidates λ_j and implement a frequency domain output-error optimization to obtain the correct modeshape $[R_j]_{NS\times NA}$ and residual terms E, F (see [2] or the similar work [3])

$$\min_{R_j,E,F} \sum_{j,k,l=1}^{NS,NA,NW} \left(H_{jk(\mathtt{id})}(\omega_l, p) - \left(\sum_{j\mathtt{id}} \left(\frac{[R_j]}{s-\lambda_j} + \frac{[\bar{R}_j]}{s-\bar{\lambda}_j} \right) + [E] + \frac{[F]}{s^2} \right) \right)^2 \tag{1}$$

and it is thus interesting to qualify the accuracy of each component in the estimated modeshape residual matrix R_j [4].

In the considered case study, accelerometers where kept fixed and 6 locations were considered for hammer impacts. Considering the first 3 locations which correspond to x, y, z directions in a single point in space, the columns of R_j give distinct estimates of modeshapes at sensors. Figure 2 illustrates that superposition is quite good, but some input/output pairs are not properly measured (here the red lines which correspond to 36z and 39z output for 13y input).

#	2	#	3	#	5	#	7	#	10	#	11	#	12	#	13
28:2	97	13:3	99	36:2	96	10:3	97	32:3	92	39:2	87	22:3	68	13:2	90
11:2	98			38:2	96	1:3	97	35:3	94	22:2	89	13:3	80	24:2	91
13:2	98			40:2	97	24:3	98	22:3	95	38:2	91	2:3	86	21:2	92
2:2	98			10:2	97	32:3	98	16:3	96	5:2	92	5:3	88	38:2	93
24:2	98			1:2	97	36:3	98	40:3	97	1:2	92	24:3	89	5:2	94

Table 1: Output (number):input number pairs leading to identification problems

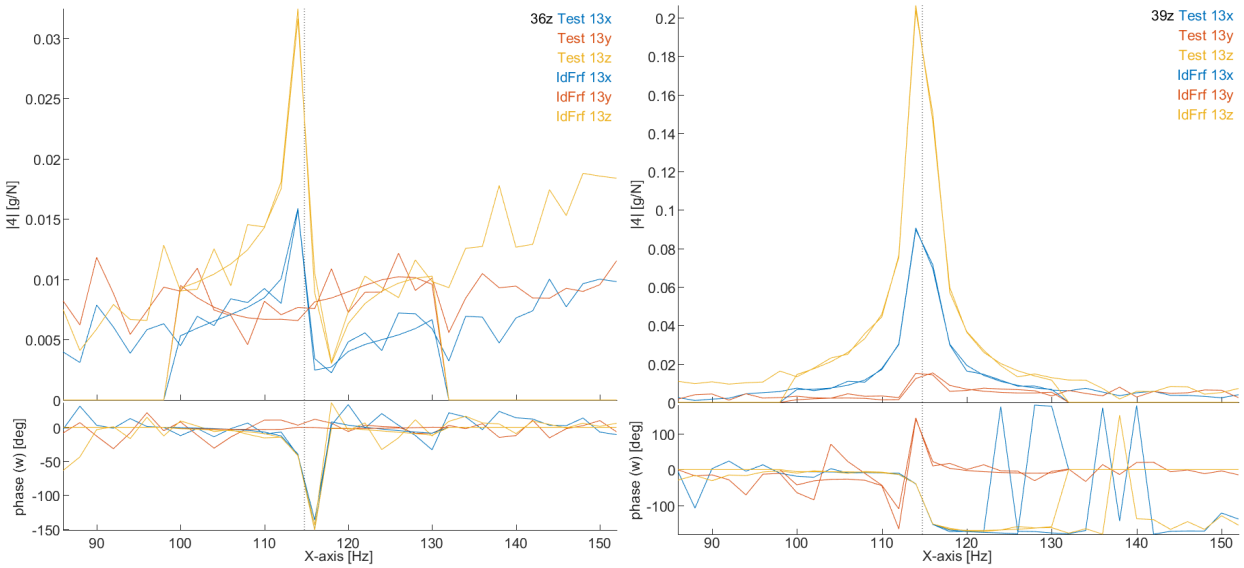

Figure 2: Selected transfer functions in the vicinity of the first mode (torsion)

As looking at individual transfers is difficult, table 1 displays the MACCo for modeshapes estimated using either MIMO cite or SIMO procedures (keeping individual columns of R_j). The table clearly indicates that a few sensors lead to poor correlation. For example for mode 12, removing sensor 22 associated with input 3(z) makes raises the MAC from 68% to 80%. In general the table also indicates that inputs in the y direction are often problematic: for modes 2, 5, 11 and 13 all sensors leading to poor correlation are in that direction. These difficulties are easily related to the low response level for y inputs. Figure 3 indeed shows that the sum of imaginary parts for y input (shown as 2 in red), has a level that is lower by a factor of at least 100 for many modes (1,2, ...).

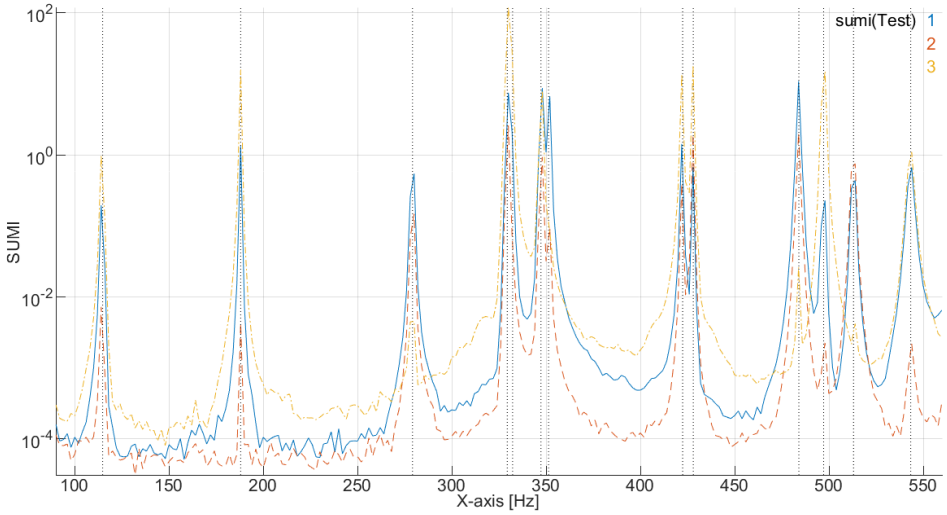

Figure 3: Sum of imaginary parts of transfer as an indication of modal commandability level.

As complementary data, the mode indicator functions [5] shown in Figure 4 indicate the presence of a missing mode near 352 Hz in the initial identification and in the left figure corresponding to the test of a component where the wide minima cannot correspond to modal resonances and thus give a direct indication of a non-linearity.

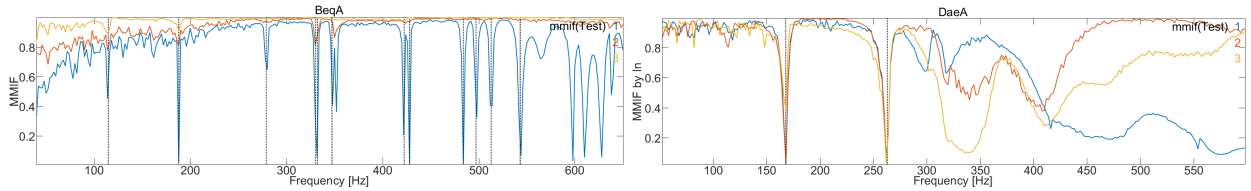

Figure 4: MIMMO MMIF for cradle (left) and component with internal non-linearities

Typical sources of problematic input/output transfers are hardware faults and noisy channels (affects all modes on a given channel), poor excitation of specific modes (affects specific modes on specific channels), non-linearity (affects specific modes on all channels). Overall, procedures to eliminate poorly identified modal components provide an initial cleanup of the test which in the present case can notably improve specific MAC values, as shown in table 1.

2.2 Localization of problematic sensors

When performing modal tests, the spatial localization of sensors remains a difficulty. Recent scanning vibrometer systems include geometric measurements, but with accelerometers the existing techniques (laser or acoustic emission triangulation, printed targets associated with photogrammetry) are not widely distributed so that errors on positioning or cabling are still a fairly common problem. In the present case study, two sensors were permuted and demonstrating that such configurations can be easily identified seems useful.

The MACCo procedure is a what-if analysis. For each mode, the MACCo at step 1 gives the sensor which contributes most to the poor correlation and the MAC when this sensor is removed. Thus the initial correlation of mode 1 is 88%, but if sensor **35z** is removed this correlation goes up to 92%. The table clearly indicates multiple occurrences of problems related to sensors 35z and 36z. Manual analysis could then pinpoint the fact that sensors were permuted and correlation of the first model went after permutation from 88% to 97%.

#	1	#	2	#	3	#	4	#	6	#	8	#	9
	88		82		84		44		48		46		69
35z	92	32z	84	17z	85	**36z**	55	28z	54	**36z**	56	4z	74
36z	94	40z	86	14z	86	**35z**	63	7z	59	7z	62	32z	79
28z	95	**36z**	88	**36z**	87	6z	68	10z	63	6z	65	24z	81
26z	96	28z	89	22z	87	39z	71	34z	67	**35z**	68	21z	83
31z	97	6z	90	26z	88	22z	74	9z	69	8z	72	3z	85

Table 2: MACCo per mode for the relevant mode pairs of the initial models

2.3 Using expansion for further analysis

Once data associated with problematic actuator/sensor pairs eliminated, the test data can be considered as valid and localization of sensors contributing to poor correlation makes sense. In the test case, the number of sensors shown in figure 5 is relatively coarse compared to the shapes of interest.

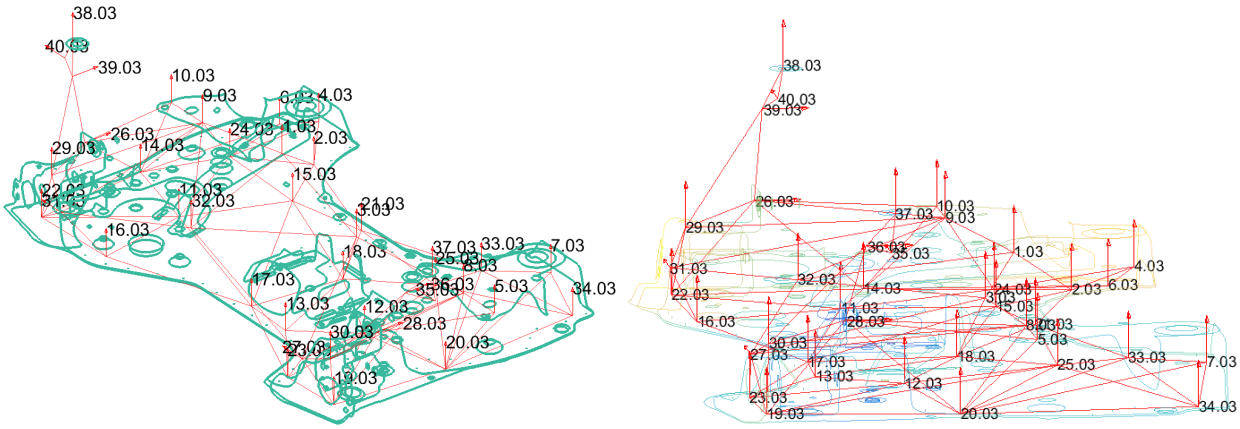

Figure 5: Position of sensors with orientations

It is thus quite useful to use modeshape expansion [6, 7]. In the present case, static expansion was used but reduced basis dynamic expansion is usually preferred. Viewing of expanded modeshapes was in particular useful to identify problems with motion at the rear (sensors 6z, 7z) which regularly appeared in the MACCo classification table 2.

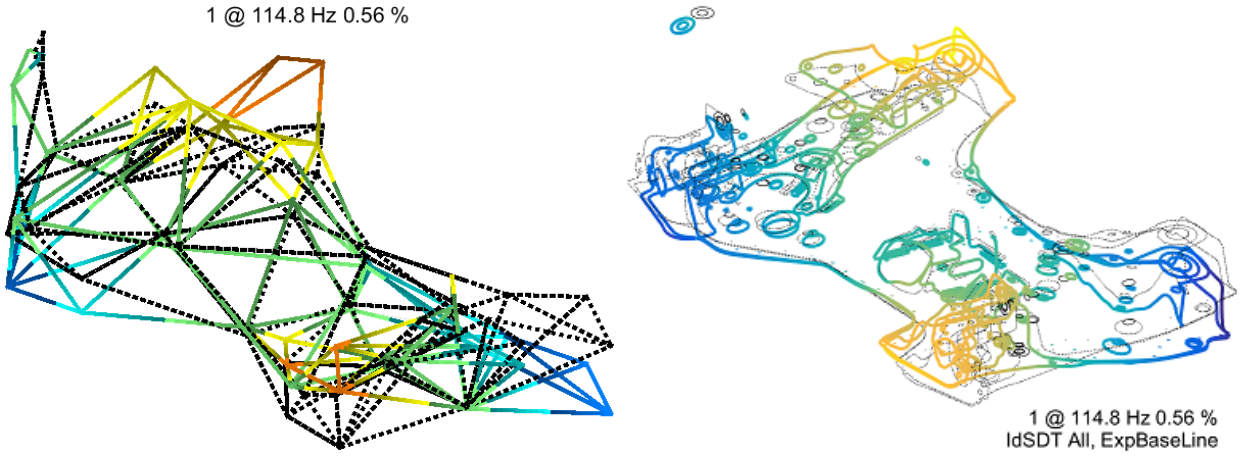

Figure 6: First mode shape using wire frame and expansion on mesh edges

3 Model parameter selection and updating

The initial guesses for influential parameters were weld spots, weld beads and thickness variations due to stamping. Sensitivity studies summarized in sections 3.1- 3.3 illustrated visible but fairly limited effects. In a second phase, it was recognized that while a number of surfaces are nominally in contact the CAD geometries, the actual contacting surfaces is subject of discussion. Section 3.4 thus proposes a strategy to analyze the impact of surface contacts. Finally, the assembly of components typically requires a number of smaller adaptation parts and the impact of possible choices is discussed in 3.5.

3.1 Weld spots

The representation of weld spots has been the object of many studies and it seems obvious some level of adapted meshing procedure is needed [8]. When a given level of refinement is chosen, updating may require a validation that the strategy chosen is sufficient for the current objective. In the present case, the initial model was a mesh with nodes at the center of each weld spot connecting the two welded surfaces by a beam and using modified properties. As this strategy is not guaranteed to properly account for the diameter of the melted zone, an automated remeshing strategy was implemented following the procedure highlighted in figure 7.

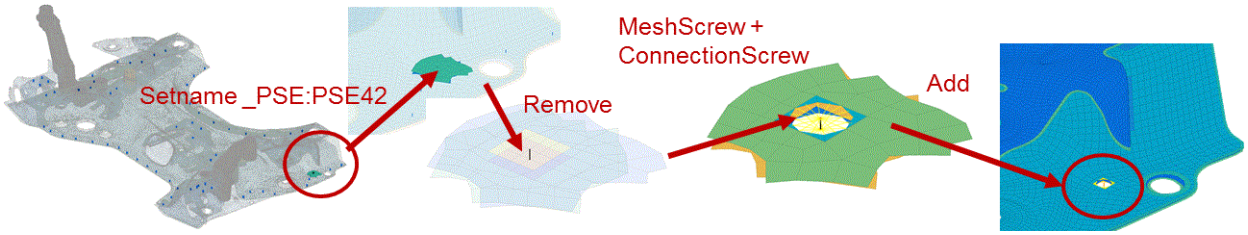

Figure 7: Automated mesh adaptation strategy for weld spots

To help localize which weld spots might need remeshing, a classification of energy contributions provides a simple view illustrated in figure 8. For each weld spot, considering the beam energy only is not easily viewed and does not account for the fact that local deformation may play a role. The energy within the neighborhood of each weld spot is thus summed and shown as a flat color in the figure. For the first mode chosen as illustration in figure 8, most of the energy is concentrated in only four weld spots (top left, middle, ...). For the second the connections of the horns are major contributors.

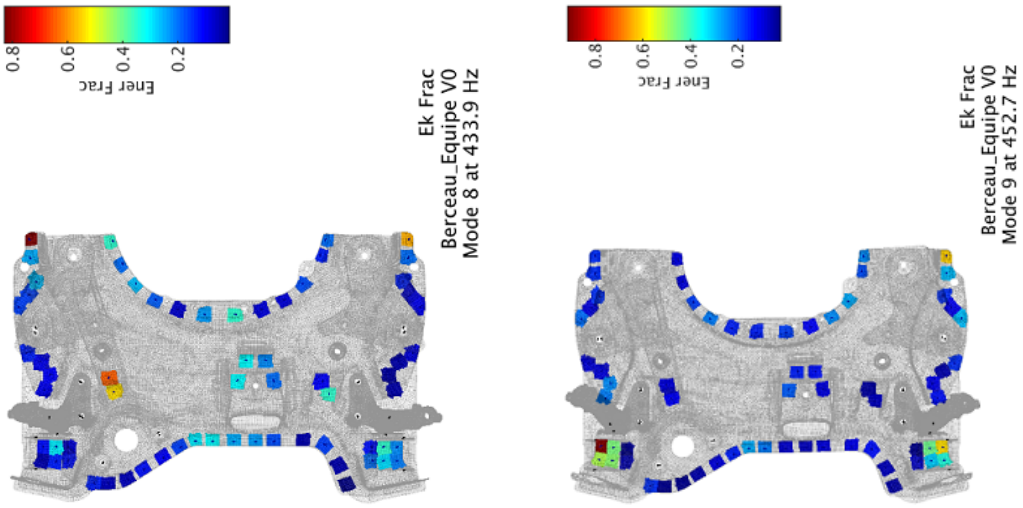

Figure 8: Energy localization around weld spots

To evaluate the validity of a given model. The proposed procedure is to use energy distribution to select weld spots of interest and then perform a selective remeshing study. As was illustrated in figure 7 this can be performed, while keeping both a great part of the mesh and possibly using the CMT (component mode tuning procedure [9]) to avoid recomputing the full FEM solution. Figure 9 top illustrates that remeshing weld spot 42 leads to a 2% shift in frequency. As the weld spot is on the right, the local bending that occurs can indeed be expected to be quite sensitive. In terms of modeshapes, this induces modal crossing which can be seen in the MAC plot at the bottom.

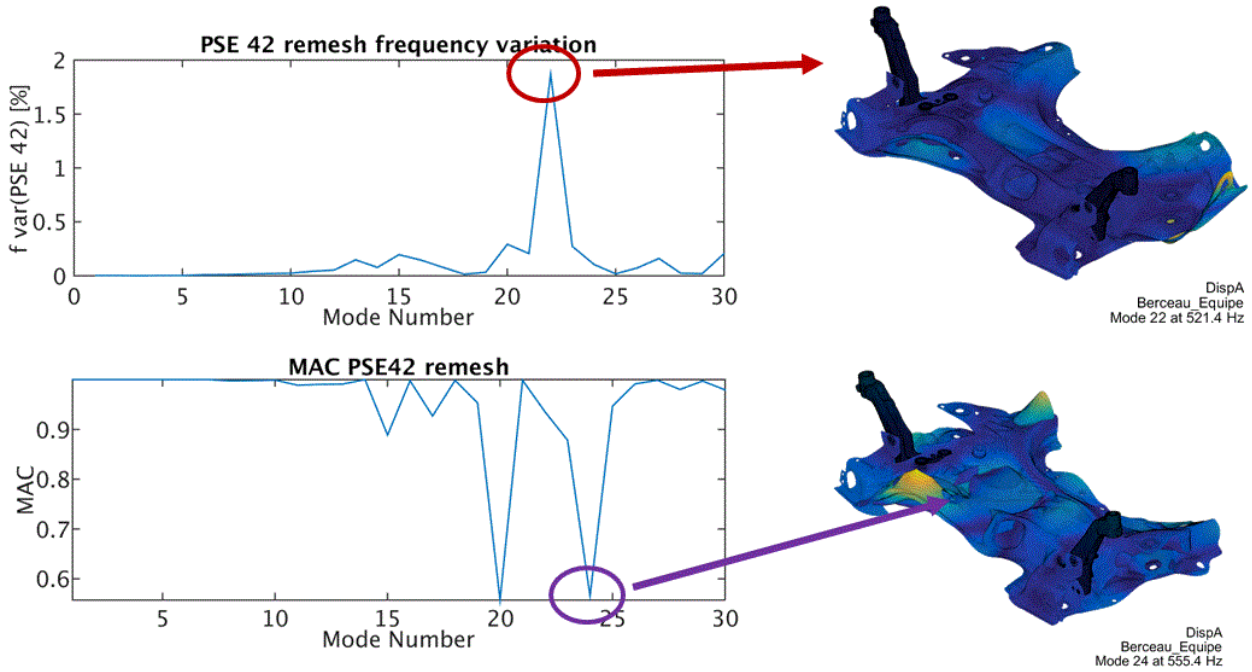

Figure 9: Sensitivity of frequencies and shapes to remeshing of PSE 42

3.2 Weld beads

For weld beads similar issues can be found. As, automotive body models typically use shell models, figuring out the effect of local flexibility may not be obvious. The proposition made is thus to locally replace the shell model by volume representations. A typical connection of the shell model is illustrated in figure 10 left and volume morphing capabilities of SDT are used to generate the topologically equivalent volume mesh on the right.

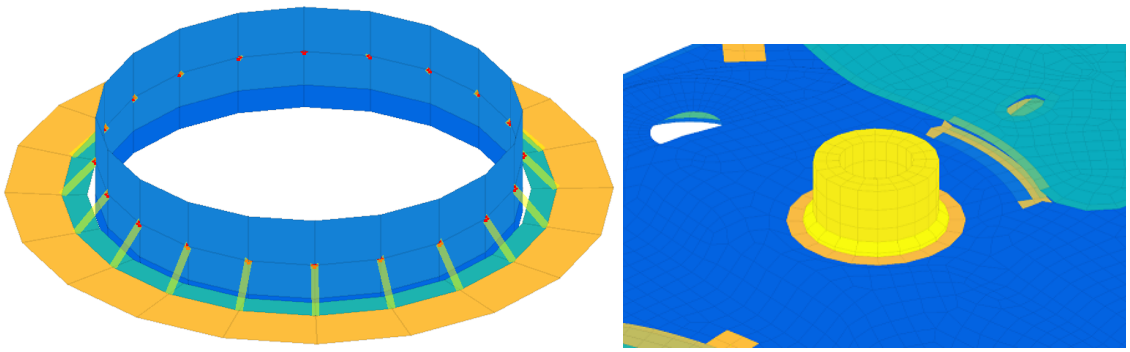

Figure 10: Shell and volume representations of a plate/cylinder welded connection

In the present case, figure 11 illustrates that relatively minor frequency shifts are found. This particular

junction is however a connection for the power-steering equipment and the influence of the junction should be reevaluated with the power-steering model connected to the cradle.

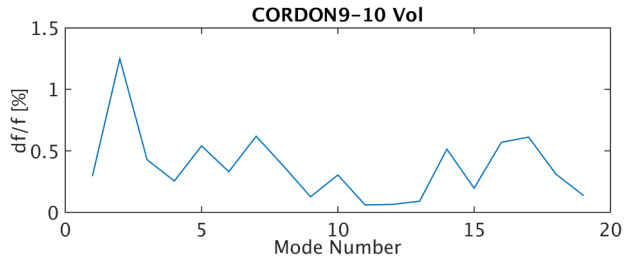

Figure 11: Influence of volume remeshing of a weld bead

3.3 Stamping

Another problem classically seen as a source of poor correlation is the fact that press forming of parts generates variations in thickness. Figure 12 illustrates the result of a press forming computation performed with AutoForm. The first difficulty of such result is that the mesh needed for relevant press forming differs from the mesh used for vibroacoustic model generation. A phase of field projection is thus needed to generate a model with variable thickness. Figure 12 right shows the end result implemented in the SDT shape optimization routines. Fo easier export to NASTRAN, the thickness values a discretized and twenty thickness are defined.

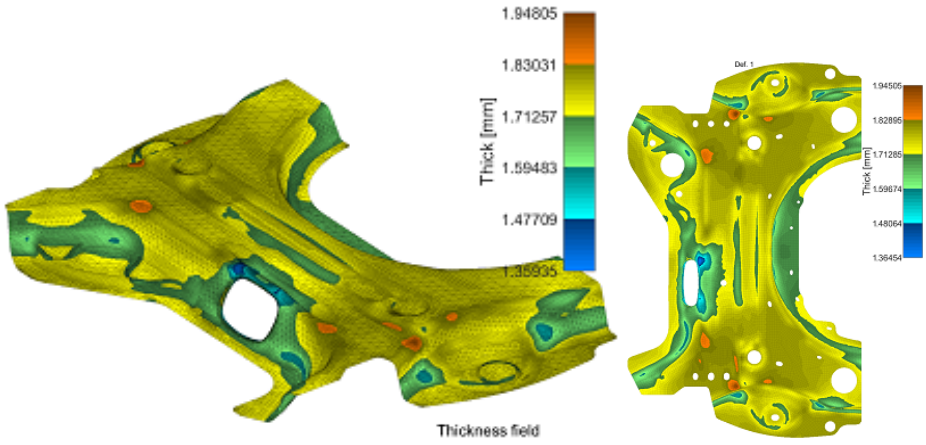

Figure 12: AutoForm prediction of final thickness values and field projection by SDT ShapeOptim to generate a NASTRAN model with thickness zones

Frequency variations associated with the thickness changes are fairly minimal (below 0.4%) and the only notable change on shapes is associated with the coupling of two close modes.

3.4 Contacting surfaces

In a large number of configurations, body parts are welded assemblies press formed parts. Figure 13 illustrates the two main parts of the engine cradle before welding. As shown by the red and orange dots on the right image, large surfaces are in contact in the CAD definition of these parts. It thus seems quite relevant to evaluate the impact that partial contact might have. The procedure used here [11] considers parametric eigenvalue problems of the form

$$\left(-\omega_j^2\left[M\right]+\left[K_e\right]+\alpha_n\left[K_n\right]+\alpha_t\left[K_t\right]\right)\left\{\phi_j(\alpha_n,\alpha_t)\right\}=0 \tag{2}$$

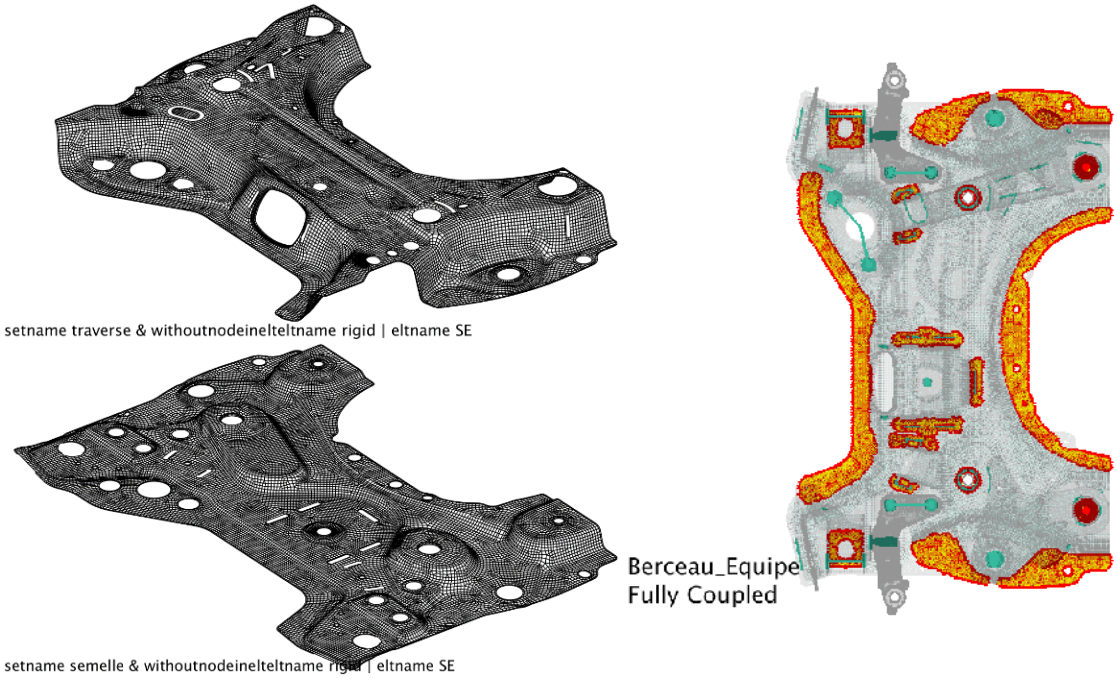

Figure 13: Engine cradle parts to be welded (left) and potential contact area (right).

Figure 14 illustrates MAC computations for baseline and fully coupled models. It clearly appears that assuming non sliding contact on the full potential surface has a major effect both on modeshapes and frequencies (up to 30%).

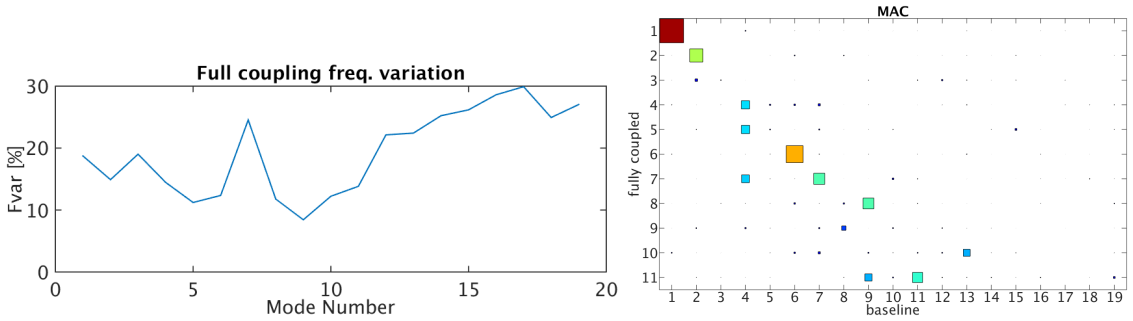

Figure 14: Frequency evolution and MAC comparison of baseline/fully coupled modeshapes

To ease this analysis, the strategy used here consists in a parametric study on the normal (contact) and tangent (sticking) stiffness. Figure 15 shows the global sensitivity curves for all modes and zooms on specific areas. In the zooms, the makers □ for normal stiffness and △ for tangent stiffness, clearly indicate varying effects from mode to mode with non-constant ordering of sensitivity to contact and friction.

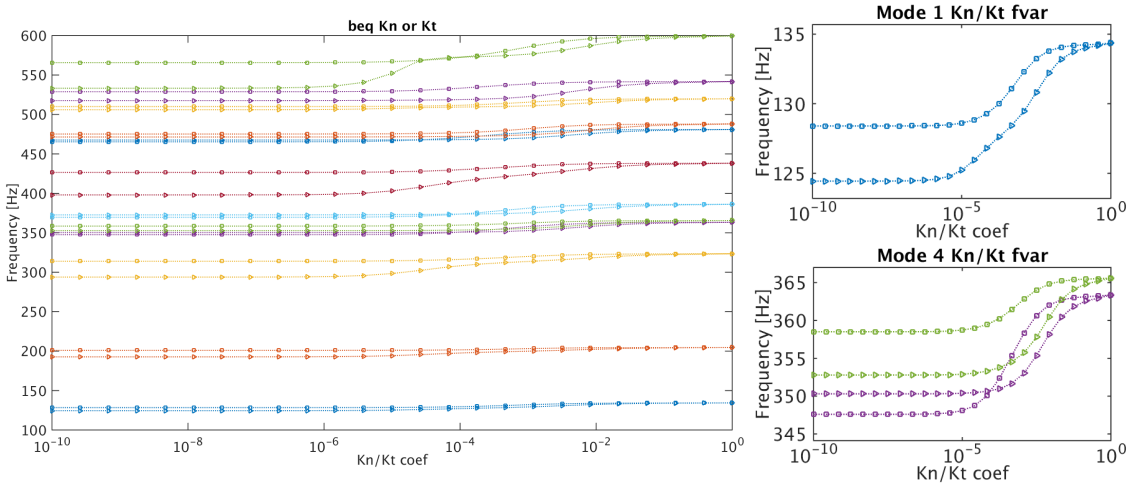

Figure 15: Engine cradle parts to be welded (left) and potential contact area (right).

A similar study was performed for the connection of horns with the potential contact surfaces shown in red in figure 16 left. The particular interest of this configuration is that it induces a number of modal crossings near 318 Hz. Mode 4 is mostly sensitive to tangent stiffness △ while mode 5 is more sensitive to normal stiffness □. The validation of such sensitivities is considered an initial step for more advanced applications where junction non-linearity and damping is considered [10].

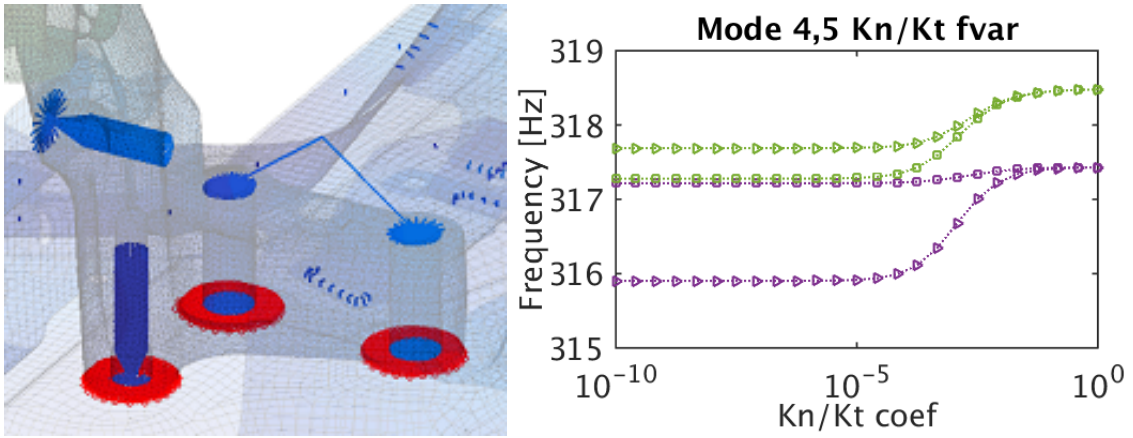

Figure 16: Potential contacts in a junction using screws. Sensitivities of selected modes 4-5.

3.5 Representation of interfaces

The next phase is to address junctions. The industrial need to specify coupling nodes, typically leads to local simplifications as illustrated in figure 17 left, were the connection point is shown in red, the mass is correctly accounted for but the ring of rigid elements stiffens the connection. The local remeshing shown on the right is geometrically more accurate and thus produces better results in terms both stiffness and mass.

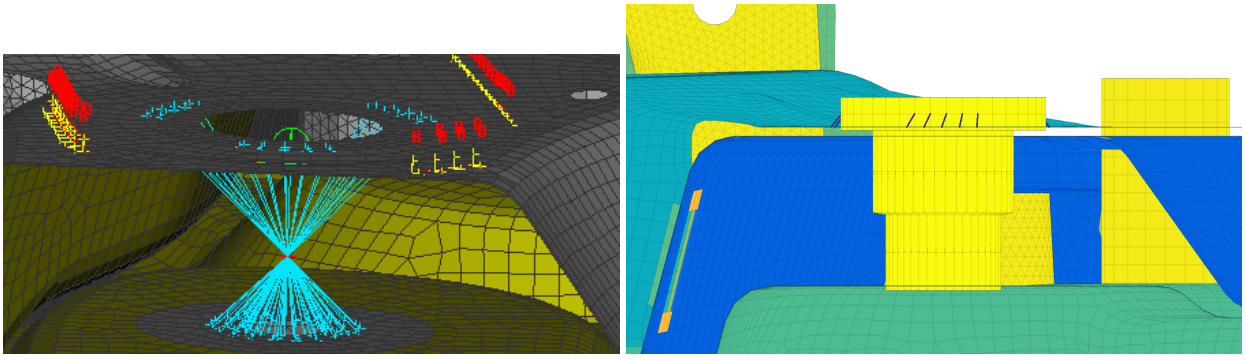

Figure 17: Rear connection of the cradle with the body.

The spacer illustrated in figure 18 illustrates another error that needed to be corrected. As the structure is quite flexible around this junction, the component test was performed by replacing the true car part by a spacer used only in the test configuration. Such fixtures are common but since they are only meant for the test, the effort in their modeling is limited. In the present case, proper modeling notably improved correlation of mode 7.

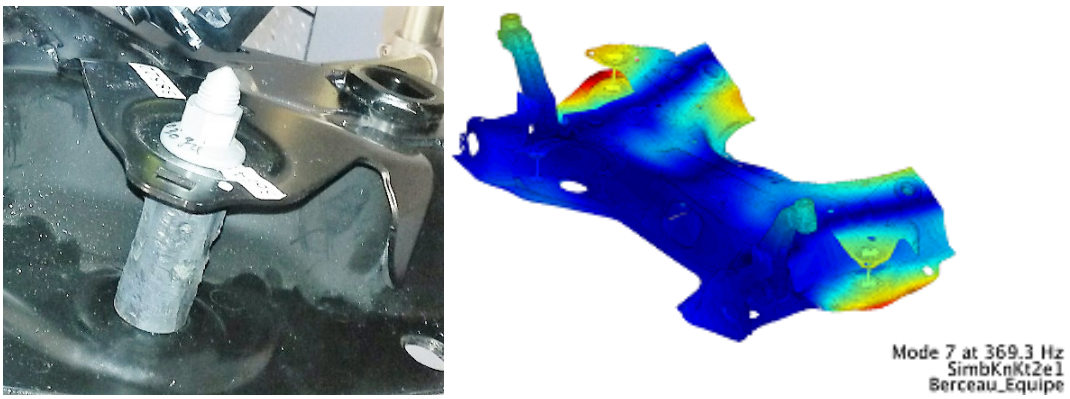

Figure 18: Spacer used specifically for the test and associated sensitive mode

4 Conclusion

This case study was a success in the sense that initial MAC values started with only 3 modes between 82% and 88% and ended with almost 8 correlated modes with more accurate frequencies. The first level of correction was just an elimination of experimental errors and procedures were proposed for this purpose.

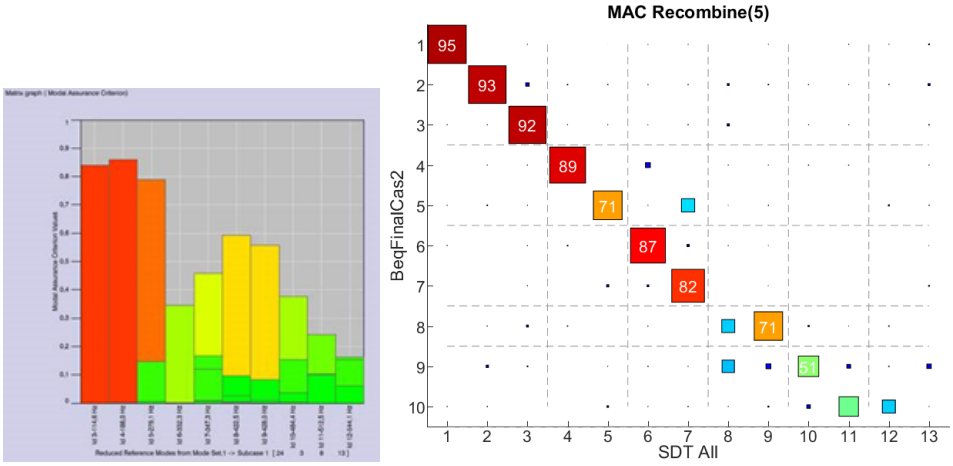

Figure 19: Initial and final shape correlation.

Modeling was addressed next. Contrary to the initial proposition, weld spots and beads as well as thickness variations due to press forming were shown to have relatively minor impact on the modal properties. Key factors in the representation were actually the poor knowledge of the surfaces actually in contact in a spot welded assembly and the simplified representation of smaller parts used for connections to the rest of the body.

The main propositions for future applications were:

- Stiffness variations due to the exact definition of contacting surfaces play a dominant role both in junctions and welded surfaces. The initial selection of parameters (part thickness, weld spot/bead stiffness) has a much lower impact. Development of testing strategies (through the thickness wave propagation for example) to clarify the actual surfaces thus seem a major need. It is also reminded that any junction showing energy is a good candidate for damping treatments [11].
- The validation of part masses is critical and in particular screws and spacers have non negligible inertia and stiffness effects at higher frequencies.
- The common strategy of using rings of rigid links tends to give unreliable results when flexibility starts to play a role. This tends to be the case at higher frequencies. A preferable approach would be to develop local modeling approaches allowing the use of physical geometries and material properties. To avoid notable increases in model size due to these local refinements, it is possible to consider couple the local mesher with a FEM solution to generate a reduced model.
- Automated updating of parameters in the presence of existing errors leads to bias. In the present case, insufficient contact stiffness was in part hidden by inconsistencies on masses.
- While the model is reasonably fine, it should be noted that dependence to element formulation is still found (coupled or lumped mass, handling of shell normals, software SDT/NASTRAN/Abaqus, ...). It must thus be understood that parameter update results would be equivalent parameters depending on model choices and not fully physical values.

Acknowledgements

PSA Peugeot Citroen provided the data for the illustration and funding for the project.

References

[1] E. Balmes, *Structural Dynamics Toolbox (for use with MATLAB)*. SDTools, Paris, September 1995-2014. [Online]. Available: http://www.sdtools.com/help/sdt.pdf

[2] ——, "Frequency domain identification of structural dynamics using the pole/residue parametrization," *International Modal Analysis Conference*, pp. 540–546, 1996. [Online]. Available: http://www.sdtools.com/pdf/IMAC96id.pdf

[3] M. El-Kafafy, B. Peeters, P. Guillaume, and T. De Troyer, "Constrained maximum likelihood modal parameter identification applied to structural dynamics," *Mechanical Systems and Signal Processing*, 2015. [Online]. Available: http://www.sciencedirect.com/science/article/pii/S0888327015004902

[4] G. Martin, E. Balmes, and T. Chancellier, "Improved Modal Assurance Criterion using a quantification of identification errors per mode-sensor," Leuven, Sep. 2014. [Online]. Available: http://hdl.handle.net/10985/8592

[5] R. Williams, J. Crowley, and H. Vold, "The Multivariate Mode Indicator Function in Modal Analysis," *International Modal Analysis Conference*, pp. 66–70, 1985.

[6] E. Balmes, "Review and Evaluation of Shape Expansion Methods," *International Modal Analysis Conference*, pp. 555–561, 2000. [Online]. Available: http://www.sdtools.com/pdf/IMAC00exp.pdf

[7] D. Kammer, "Sensor set expansion for modal vibration testing," *Mechanical Systems and Signal Processing*, vol. 19, no. 4, pp. 700–713, 2005. [Online]. Available: http://dx.doi.org/10.1016/j.ymssp.2004.06.003

[8] S. Donders, M. Brughmans, L. Hermans, C. Liefooghe, H. Van der Auweraer, and W. Desmet, "The robustness of dynamic vehicle performance to spot weld failures," *Finite Elements in Analysis and Design*, vol. 42, no. 8–9, pp. 670–682, May 2006. [Online]. Available: http://www.sciencedirect.com/science/article/pii/S0168874X05001447

[9] G. Vermot des Roches, J.-P. Bianchi, E. Balmes, R. Lemaire, and T. Pasquet, "Using component modes in a system design process," in *International Modal Analysis Conference*, 2010, pp. 1–2. [Online]. Available: http://www.sdtools.com/pdf/imac10_component.pdf

[10] G. Vermot Des Roches and E. Balmes, "Understanding friction induced damping in bolted assemblies through explicit transient simulation," in *ISMA*. KUL, Sep. 2014, p. ID360. [Online]. Available: https://hal.archives-ouvertes.fr/hal-01066967/document

[11] C. Hammami, E. Balmes, and M. Guskov, "Numerical design and test on an assembled structure of a bolted joint with viscoelastic damping," *Mechanical Systems and Signal Processing*, vol. 70–71, pp. 714–724, Sep. 2015.